HYBRID MODAL & METHOD-OF-MOMENTS ANALYSIS OF THE INTERACTION BETWEEN A GTEM-CELL AND A DEVICE UNDER TEST

Michael Zellerhoff [(1)], Ludger Klinkenbusch [(2)]

Computational Electromagnetics Group, University of Kiel, Kaiserstraße 2, 24143 Kiel, Germany

[(1)] E-mail: zellerhoff@ieee.org
[(2)] E-mail: lbk@cem.tf.uni-kiel.de

MOTIVATION

The contribution deals with the efficient numerical evaluation of the electromagnetic field within a semi-infinite tapered TEM-waveguide partially filled with an arbitrary object. The investigation of this problem is mainly motivated by the benefit which could arise from a systematic study of this class of geometries for the judgement of the reliability of so-called GTEM cells; these are widely used in EMC practice for the measurement of both the electromagnetic emission from and the susceptibility of relatively small devices under test (DUT). Since such GTEM cells promise to work up to frequencies in the GHz region, and their dimensions are about 6 meters in length, a purely numerical method is expensive and, as will be shown, unnecessary. Moreover the proposed hybrid modal-analysis & Method-of-Moments approach could be of general interest for the efficient simulation of mainly homogeneous waveguides that have an arbitrary inhomogeneous part.

FORMULATION AND SOLUTION OF THE BOUNDARY-VALUE PROBLEM

As a first step the two-dimensional problem is treated: Consider a perfectly electrically conducting (PEC) DUT, located in the interior of a wedge with PEC walls, where the DUT, the wedge and a (line) source distribution do not depend of the direction parallel to the wedge's edge. This two-dimensional problem is well suited for the evaluation of the algorithm. Moreover, it allows an insight into the processes within such a cell; in particular the undesired interaction between the cell and the DUT can be studied systematically. It is noted that the method can be generalized to the three-dimensional case, e.g., while treating a conical TEM-waveguide with elliptic cross-section and a sector-like inner conductor.

There is only a very small part of the cell occupied by the DUT, while the main part is empty. To take advantage of this fact, we first split the cell into three domains as shown in Fig. 1.

Using a plane polar coordinate system (R, φ) with the origin at the wedge's edge, the domains I, II and III are defined as seen from Fig. 1. Domains I and II are empty, while domain III surrounds the DUT. The electromagnetic field component perpendicular to the shown plane is denoted by Ψ and must satisfy the scalar Helmholtz equation within the domains and the Dirichlet- or the Neumann condition at the metallic boundaries. Furthermore, Ψ has to be continuous through the interfaces C_1 and C_2 between the domains. A time factor $e^{+j\omega t}$ is assumed and omitted throughout the analysis.

For Part I and II of the cell, we describe Ψ by means of a modal analysis

$$\Psi^{I}(\vec{R}\,) = \sum_{n=0}^{\infty} a_n^{I\,inc} H^{(2)}_{\frac{n\pi}{\alpha}}(\kappa R) \begin{matrix}\sin\\ \cos\end{matrix} \left(\frac{n\pi}{\alpha}\varphi\right) + \sum_{n=0}^{\infty} a_n^{I\,sc} H^{(1)}_{\frac{n\pi}{\alpha}}(\kappa R) \begin{matrix}\sin\\ \cos\end{matrix} \left(\frac{n\pi}{\alpha}\varphi\right) \tag{1}$$

$$\Psi^{II}(\vec{R}\,) = \sum_{n=0}^{\infty} a_n^{II\,inc} H^{(1)}_{\frac{n\pi}{\alpha}}(\kappa R) \begin{matrix}\sin\\ \cos\end{matrix} \left(\frac{n\pi}{\alpha}\varphi\right) + \sum_{n=0}^{\infty} a_n^{II\,sc} H^{(2)}_{\frac{n\pi}{\alpha}}(\kappa R) \begin{matrix}\sin\\ \cos\end{matrix} \left(\frac{n\pi}{\alpha}\varphi\right), \tag{2}$$

where the sine- and the cosine functions are to be used for the Dirichlet- and for the Neumann case, respectively. $H^{(1)}_{\frac{n\pi}{\alpha}}$ and $H^{(2)}_{\frac{n\pi}{\alpha}}$ represent Hankel functions of the first and second kind, respectively, and $\kappa = \omega\sqrt{\varepsilon_0\mu_0}$ is the free-space wave

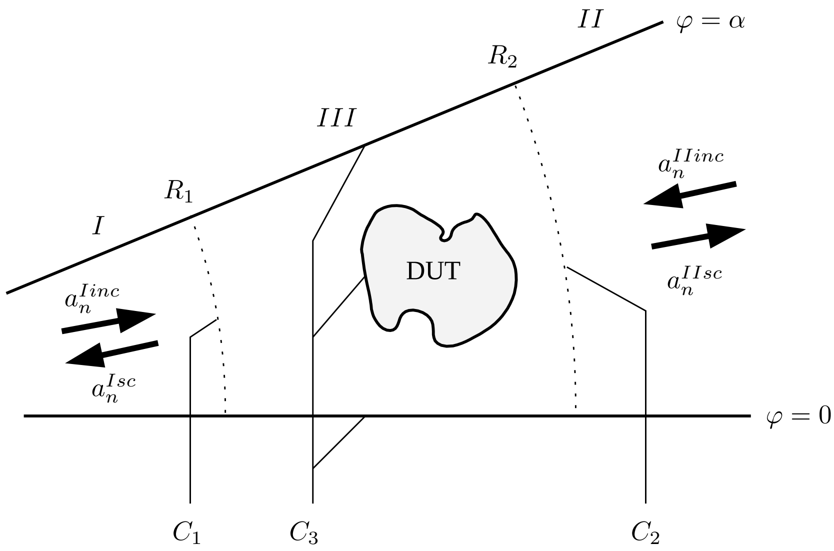

Fig. 1: Subdivision of the cell

number. $a_n^{I\,inc}$ and $a_n^{II\,inc}$ are the known amplitudes of the incident fields, whereas the amplitudes $a_n^{I\,sc}$ and $a_n^{II\,sc}$ of the scattered fields are to be determined. While exploiting Green's second identity and provided that there are no sources within domain III (susceptibility test) we represent Ψ within domain III by

$$\Psi^{\mathrm{III}}(\vec{R}\,) = \oint\limits_C \left[G(\vec{R}\,,\vec{R}\,')\,\frac{\partial}{\partial n'}\Psi^{\mathrm{III}}(\vec{R}\,') - \Psi^{\mathrm{III}}(\vec{R}\,')\frac{\partial}{\partial n'}G(\vec{R}\,,\vec{R}\,')\right] ds', \tag{3}$$

where $C = C_1 + C_2 + C_3$, $\hat{n}'$ is the normal outward-directing unit vector on C and $G(\vec{R}\,,\vec{R}\,')$ denotes the free-space Green's function. If the field point in (3) matches the boundary C, we obtain a field integral equation. Since in the Dirichlet case it holds $\Psi^{III}\big|_{\vec{R}\in C_3} = 0$ and in the Neumann case we have $(\partial/\partial n')\Psi^{III}\big|_{\vec{R}\in C_3} = 0$, on the boundary C_3 only one part of the two in the integrand of (3) is non-zero in each case; the unknown in the other part is approximated by a set of sub-domain basic functions. On C_1 and C_2, Ψ^{III} and $(\partial/\partial n')\Psi^{III}$ are due to the continuity conditions obtained directly as Fourier series from (1) and (2).

Using the MoM we transform the problem into a matrix equation ([1, 3, 4]. If the coupling integrals involve only the sub-domain expansions on C_3, the closed form of the free-space Green's function

$$G(\vec{R}\,,\vec{R}\,') = \frac{1}{4j}H_0^{(2)}\left(\kappa\left|\vec{R} - \vec{R}'\right|\right) \tag{4}$$

is employed; the testing on C_3 is performed with usual point-matching. For the evaluation of the coupling integrals involving C_1 and C_2 we use the modal expansion of the free-space Green's function

$$G(\vec{R}\,,\vec{R}\,') = \frac{1}{4j}\left[J_0(\kappa R_<)H_0^{(2)}(\kappa R_>) + 2\sum_{n=1}^{\infty} J_n(\kappa R_<)H_n^{(2)}(\kappa R_>)\cos n\,(\varphi - \varphi')\right], \tag{5}$$

where the abbreviations

$$R_< = \min(R, R')\,; \quad R_> = \max(R, R') \tag{6}$$

are introduced. The testing on C_1 and C_2 is done due to the Galerkin formalism, that is, test functions $\cos\frac{n\pi}{\alpha}\varphi$ and $\sin\frac{n\pi}{\alpha}\varphi$ are employed. This procedure allows an analytical evaluation of the related integrals. The series' convergence is ensured because of the behaviors of the Bessel functions and of the coupling integrals. The numerical solution of the obtained system of linear equations yields the coefficients of the sub-domain basis functions on C_3 and, directly, the scattered-field's modal coefficients $a_n^{I\,sc}, a_n^{II\,sc}$ in (1) and (2).

VALIDATION AND NUMERICAL RESULTS

The consistency of the proposed method has been successfully validated for the case of an empty cell by inserting the 'problem-adapted' Green's function of the wedge, i.e., where the boundary conditions on C_3 are automatically fulfilled

$$G(\vec{R},\vec{R}\,') = \frac{\pi\epsilon_n}{4j\alpha}\sum_{n=0}^{\infty} J_{\frac{n\pi}{\alpha}}(\kappa R_<)H^{(2)}_{\frac{n\pi}{\alpha}}(\kappa R_>)\,\begin{matrix}\sin\\ \cos\end{matrix}\left(\frac{n\pi}{\alpha}\varphi\right)\begin{matrix}\sin\\ \cos\end{matrix}\left(\frac{n\pi}{\alpha}\varphi'\right) \tag{7}$$

with

$\epsilon_n = 1$ if $n = 0$, and $\epsilon_n = 2$ if $n = 1, 2, 3, ...$

We analytically derive the expected result: $a_n^{I\,sc} = a_n^{II\,inc}$ and $a_n^{II\,sc} = a_n^{I\,inc}$. Moreover, this result is also the objective for the numerical evaluation of the empty-cell case while using the free-space Green's functions. Also, this case is well suited for numerical studies to find the optimal parameters and to estimate the number of relevant modes and sub-domain basis functions which are needed to match the desired accuracy. Moreover, it is worth noting that the attempt to employ the wedge's Green's function [7] for the general numerical solution of the problem (i.e. for the non-empty cell case as well) fails because of the missing convergence of the related series in case when the source point approaches the observation point.

The results from first studies with a cylindric DUT, symmetrically located within the domain III, are represented in Figures 2 and 3. The observed resonances are due to an interaction between the cell and the cylindrical DUT, and are obviously corresponding to the distances between the DUT and the cell's wall.

CONCLUSIONS

A hybrid method based on the modal analysis and on the method of moments is introduced which allows to efficiently compute the electromagnetic field within a homogeneous waveguide with an arbitrary inhomogeneous part. As an application, a two-dimensional model of a partially filled GTEM cell is analyzed. The interactions between the GTEM-cell walls and the DUT which are responsible for the distortion of the test-field and should be taken into consideration while using a GTEM-cell, can be studied in detail. Since this is a very fast algorithm, also simulations for the transient case can be performed while using Fourier-transform techniques. Future work will focus on a comparison between the present GTEM-results with simulated open-site results. Finally it is worth noting that the method can directly be generalized for the case of three-dimensional problems, e.g., for a conical elliptical waveguide with an inner sector-like conductor.

REFERENCES

[1] Harrington, R.F., Field Computation by Moment Methods. IEEE Press and John Wiley & Sons, New York, 1993.

[2] De Leo, R. et.al., Dipole Excitation and Scattering by Spherical Objects in GTEM cells. IEEE Trans. Microwave Theory and Techn., 42 (1994) 1700-1708.

[3] Kress, R., Linear Integral Equations, New York: Springer, 2nd ed., 1999.

[4] Morita, N., Kumagi, N. and Mautz, J. R., Integral Equation Methods for Electromagnetics, Boston: Artech House, 1990.

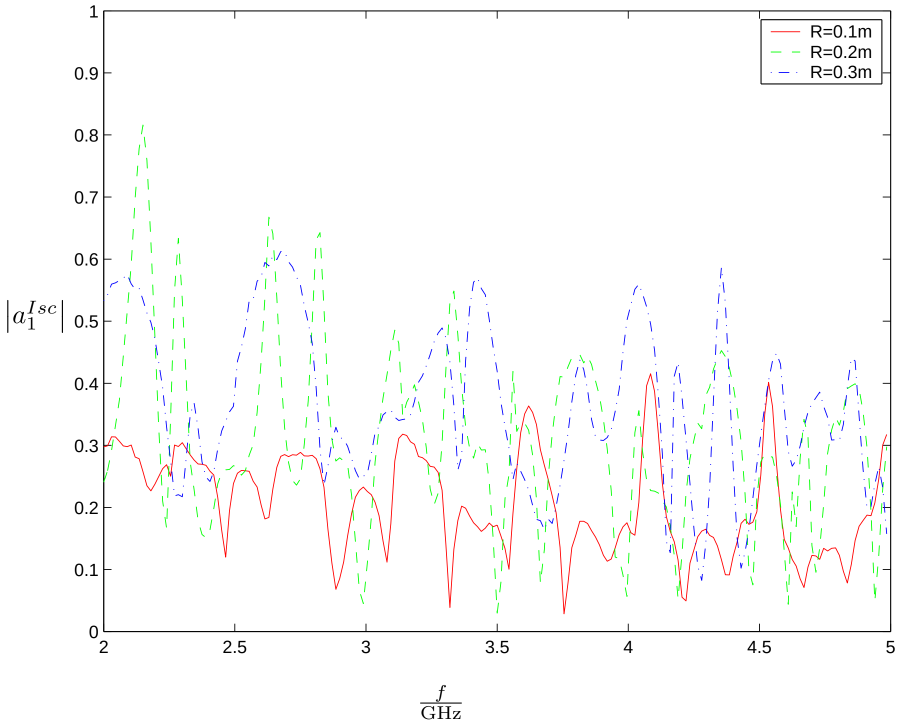

Fig. 2: Amplitude (amount) of the reflected mode $\left|a_1^{Isc}\right|$ vs. the frequency f for different radii R of the cylindrical DUT. The incident field is given by the first mode ($a_1^{Iinc} = 1$), Dirichlet case. Cell with $R_1 = 1\mathrm{m}, R_2 = 2\mathrm{m}, \alpha = 30^0$.

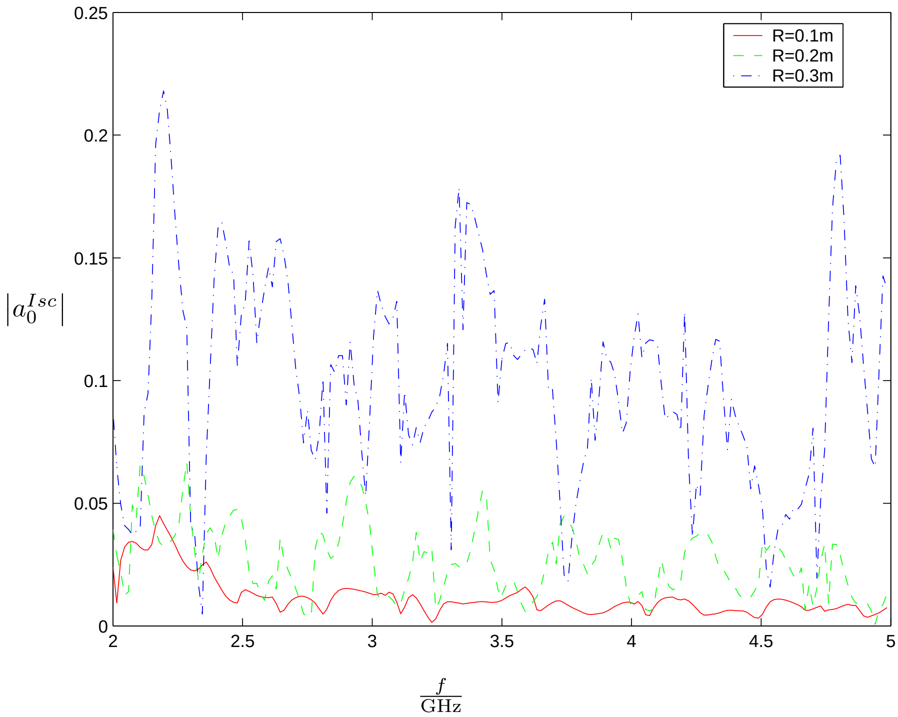

Fig. 3: Amplitude (amount) of the reflected mode $\left|a_0^{Isc}\right|$ vs. the frequency f for different radii R of the cylindrical DUT. The incident field is given by the first mode ($a_0^{Iinc} = 1$), Neumann (TEM-) case. Cell with $R_1 = 1\mathrm{m}, R_2 = 2\mathrm{m}, \alpha = 30^0$.